

Augmented Phosphorylation of Cardiac Troponin I in Hypertensive Heart Failure^{*[S]}

Received for publication, August 15, 2011, and in revised form, October 17, 2011 Published, JBC Papers in Press, November 3, 2011, DOI 10.1074/jbc.M111.293258

Xintong Dong^{†1}, C. Amelia Sumandea[§], Yi-Chen Chen[‡], Mary L. Garcia-Cazarin[§], Jiang Zhang[‡], C. William Balke[¶], Marius P. Sumandea^{§2}, and Ying Ge^{¶||3}

From the [†]Human Proteomics Program and ^{||}Department of Cell and Regenerative Biology, School of Medicine and Public Health, University of Wisconsin, Madison, Wisconsin 53706, the [§]Department of Physiology, University of Kentucky, Lexington, Kentucky 40536, and the [¶]Clinical and Translational Science Institute and Department of Medicine, University of California, San Francisco, California 94143

Background: Phosphorylation of cardiac troponin I (cTnI) is critical in modulating contractility.

Results: cTnI is hyperphosphorylated at Ser^{22/23} and Ser^{42/44} in spontaneously hypertensive rat of heart failure.

Conclusion: The augmented phosphorylation of cTnI in hypertensive heart failure is correlated with elevated protein levels of PKC- α and - δ .

Significance: This is the first *in vivo* evidence of cTnI phosphorylation at Ser^{42/44} in an animal model of hypertensive heart failure.

An altered cardiac myofilament response to activating Ca²⁺ is a hallmark of human heart failure. Phosphorylation of cardiac troponin I (cTnI) is critical in modulating contractility and Ca²⁺ sensitivity of cardiac muscle. cTnI can be phosphorylated by protein kinase A (PKA) at Ser^{22/23} and protein kinase C (PKC) at Ser^{22/23}, Ser^{42/44}, and Thr¹⁴³. Whereas the functional significance of Ser^{22/23} phosphorylation is well understood, the role of other cTnI phosphorylation sites in the regulation of cardiac contractility remains a topic of intense debate, in part, due to the lack of evidence of *in vivo* phosphorylation. In this study, we utilized top-down high resolution mass spectrometry (MS) combined with immunoaffinity chromatography to determine quantitatively the cTnI phosphorylation changes in spontaneously hypertensive rat (SHR) model of hypertensive heart disease and failure. Our data indicate that cTnI is hyperphosphorylated in the failing SHR myocardium compared with age-matched normotensive Wistar-Kyoto rats. The top-down electron capture dissociation MS unambiguously localized augmented phosphorylation sites to Ser^{22/23} and Ser^{42/44} in SHR. Enhanced Ser^{22/23} phosphorylation was verified by immunoblotting with phospho-specific antibodies. Immunoblot analysis also revealed up-regulation of PKC- α and - δ , decreased PKC ϵ , but no changes in PKA or PKC- β levels in the SHR myocardium. This provides direct evidence of *in vivo* phosphorylation of cTnI-Ser^{42/44} (PKC-specific) sites in an animal model of hypertensive heart failure, supporting the hypothesis that PKC

phosphorylation of cTnI may be maladaptive and potentially associated with cardiac dysfunction.

Heart disease is the leading cause of morbidity and mortality in industrialized societies and is becoming a worldwide epidemic (1, 2). The molecular and cellular mechanisms underlying heart failure are complex and not fully understood (2, 3). Cardiac troponin I (cTnI),⁴ the inhibitory subunit of cardiac troponin complex, is a key element in the Ca²⁺-dependent regulation of contraction and relaxation of cardiac muscle (4, 5). Since its identification in 1972 by Stull and others (6, 7), it has been widely recognized that phosphorylation of cTnI changes its conformation and modulates cardiac contractility (5, 8, 9). Altered cTnI phosphorylation status has been proposed as an underlying mechanism in heart failure (10–12).

cTnI is phosphorylated by various protein kinases, most notably protein kinase A (PKA) and protein kinase C (PKC) (8, 13–19). Extensive studies have demonstrated that PKA phosphorylates cTnI at Ser^{22/23}, generating the “fight or flight” response to β -adrenergic stimulation (8, 20). Phosphorylation at these sites reduces myofilament Ca²⁺ sensitivity and increases the cross-bridge cycling rate (8). PKC can phosphorylate cTnI at Ser^{22/23}, Ser^{42/44}, and Thr¹⁴³ (also known as Ser^{23/24}, Ser^{43/45}, and Thr¹⁴⁴ if counting the N-terminal methionine) following activation of G protein-coupled receptors by angiotensin II (AngII), endothelin-1, and the α -adrenergic agonist phenylephrine (8, 21). Ser^{42/44} and Thr¹⁴³ are traditionally viewed as PKC-specific phosphorylation sites. Phosphorylation of Ser^{42/44} (sites common for all PKC isozymes especially PKC- α) reduces the maximum Ca²⁺ activated force, Mg-ATPase rate, and cross-bridge cycling rate (8, 16, 22). Recent studies suggest that Thr¹⁴³ is a good *in vitro* substrate

* This work was supported, in whole or in part, by National Institutes of Health Grants R01HL096971 (to Y. G.) and AG032009 (to M. P. S.). This work was also supported by the Wisconsin Partnership Fund for a Healthy Future and an American Heart Association Scientist Development grant (to Y. G.).

[S] This article contains supplemental Figs. S1–S3.

¹ Present address: Dept. of Biology, Stanford University, Stanford, CA 94305.

² To whom correspondence may be sent at the present address: Eli Lilly and Company, Lilly Corporate Center, Indianapolis, IN 56285. E-mail: sumandea_marius_p@lilly.com.

³ To whom correspondence may be addressed: 1300 University Ave., SMI 130, Madison, WI 53706. Tel.: 608-263-9212; Fax: 608-265-5512; E-mail: ge2@wisc.edu.

⁴ The abbreviations used are: cTnI, cardiac troponin I; AngII, angiotensin II; ECD, electron capture dissociation; MS/MS, tandem mass spectrometry; PTM, post-translational modification; SHR, spontaneously hypertensive rat; SHR-HF, SHR with heart failure; WKY, Wistar-Kyoto rat.

for PKC- β and Tyr-phosphorylated PKC- δ (16, 19, 23, 24). PKC isozymes $\alpha/\beta/\delta$ also cross-phosphorylate Ser^{22/23} (14, 16, 19, 24). Up-regulation of PKC- α and - δ is correlated with cardiac dysfunction whereas PKC- ϵ seems to have a cardioprotective role (3, 25, 26). Whereas the functional significance of the PKA phosphorylation sites has been investigated thoroughly, the PKC phosphorylation sites in cTnI and their roles in regulation of pathophysiological cardiac function remain controversial, in part, due to the lack of *in vivo* phosphorylation evidence (27).

Top-down mass spectrometry (MS) is a powerful technique for comprehensive analysis of protein post-translational modifications (PTMs) because it can universally detect all existing modifications without *a priori* knowledge and accurately map PTM sites with full sequence coverage (28–35, 37–39). This top-down MS method eliminates the need for proteolytic digestion. Instead, it analyzes whole proteins directly in the mass spectrometer to obtain accurate molecular weight measurements of all forms of the protein in the first step. Subsequently, the modified form of the protein can be isolated in the mass spectrometer (like “gas-phase” purification) and fragmented by various tandem MS (MS/MS) techniques for reliable mapping of the PTM sites. Electron capture dissociation (ECD), a nonergodic MS/MS technique, can preserve labile PTMs during its fragmentation process and is, thus, especially suited for studying protein phosphorylation (32–34, 40). We have extensively studied the basal phosphorylation level of cTnI purified from healthy human and animal heart tissues using such a top-down approach and unambiguously identified Ser^{22/23} as the basally phosphorylated sites in human, monkey, pig, rat, and mouse cTnI (32, 33, 41, 42). Hyperphosphorylation of Ser^{42/44} and Thr¹⁴³ have not been identified in healthy hearts with normal cardiac function. Thus, a comprehensive study of endogenous cTnI modifications in animal models of heart failure is imperative to our understanding of protein kinase-dependent regulation of cardiac contractile dysfunction.

Here, we combined top-down high resolution MS/MS, affinity purification, and Western blot analysis to study the phosphorylation of cTnI in the spontaneously hypertensive rat (SHR). Since its development from Wistar-Kyoto rats (WKY) in 1963 (43), the SHR has been the most extensively studied model of hypertension-induced heart failure (43, 44). Similar to patients with hypertension, SHRs progress from persistent hypertension (at approximately 2 months of age) to stable compensated hypertrophy (at approximately 6 months of age) to cardiac dysfunction and heart failure (at approximately 18 months of age) (45). The transition from compensated hypertrophy to heart failure is accompanied by marked changes in cardiac function associated with altered mechanical properties of cardiac myofilaments. In this study, we have thoroughly characterized the PTMs of cTnI from SHR and WKY hearts. Quantitative MS and immunoblot analysis showed augmented phosphorylation of cTnI in SHRs. The top-down ECD MS/MS unambiguously mapped the up-regulated phosphorylation sites to Ser^{22/23} and Ser^{42/44}. Additionally, immunoblot analysis also revealed up-regulation of PKC- α and - δ , decreased PKC- ϵ , but no changes in PKA or PKC- β levels in the failing SHR myocardium. Our data provide direct evidence of *in vivo* hyperphosphorylation of cTnI-Ser^{42/44} sites in an animal model of

hypertensive heart failure, supporting the hypothesis that PKC phosphorylation of cTnI may be maladaptive and potentially associated with cardiac dysfunction. To our knowledge, this is the first *in vivo* evidence documenting phosphorylation of cTnI-Ser^{42/44} in a pathological condition.

EXPERIMENTAL PROCEDURES

Materials—All reagents were obtained from Sigma unless noted otherwise. Protease inhibitor mixture was purchased from Roche Diagnostics. All solutions were prepared in Milli-Q water (Millipore).

Animals and Tissue Preparation—Male SHR and WKY were purchased from Charles River or Harlan animal research laboratories. Blood pressure was monitored weekly in nonanesthetized animals by the tail cuff method. All animals were handled in accordance with the guidelines of the University of Kentucky Animal Care Committee. Left ventricular tissues were prepared from hearts of 5-week-old and 80-week-old SHRs and age-matched WKY controls. SHR and WKY hearts were removed quickly under deep anesthesia (sodium pentobarbital, 100 mg/kg intraperitoneally) and rinsed free of blood in ice-cold saline (0.9% NaCl) or Tyrode's buffer. The tissues were immediately snap-frozen in liquid nitrogen and stored at -80°C .

Western Blot Analysis—Left ventricular tissue was minced into small pieces and homogenized in a Dounce homogenizer in ice-cold buffer containing 75 mM KCl, 10 mM imidazole (pH 7.2), 2 mM MgCl₂, 2 mM EGTA, 1 mM NaN₃, 1 M DTT, 1% Triton X-100, and a mixture of protease and phosphatase inhibitors, as reported previously (46). Triton X-100 was omitted from preparations used to determine PKA expression levels (47). Isolated myofibrils were suspended in a urea-thiourea loading buffer, resolved by 12.5% SDS-PAGE, transferred to a Hybond-LF membrane (GE Healthcare), blocked for 1–2 h at room temperature in 5% ECF blocking agent (GE Healthcare) and incubated with the following primary antibodies: anti-PKA (BD Transduction Laboratories), anti-actin (Sigma), anti-cTnI-Ser^{22/23} (Cell Signaling Technology), anti-cTnI (Fitzgerald Industries, Acton, MA) and anti-PKC α , - β , - δ , and - ϵ (Cell Signaling Technology or Santa Cruz Biotechnology). Membranes were then incubated for 1 h at room temperature with anti-rabbit or anti-mouse IgG alkaline phosphate-conjugated secondary antibody. Protein bands were detected using ECF substrate (GE Healthcare). Membranes were scanned using a Typhoon-9410 (GE Healthcare). Scans were analyzed using ImageQuant TL software.

Immunoaffinity Chromatography—The cTn complexes were purified from left ventricles of individual rat hearts by immunoaffinity chromatography as described previously (10, 33, 41, 48) with minor modifications (42, 49). The entire purification process was conducted at 4°C to minimize the enzymatic activity and preserve the endogenous state. The cTn complex was eluted from CNBr-activated Sepharose CL-4B conjugated with an anti-troponin I monoclonal antibody (MF4; Hytest) with 100 mM glycine HCl (pH 2). A total of 6–7 eluted samples with 400 ml each were collected into 1.5-ml microcentrifuge tubes containing 40 ml of MOPS (pH 9). The flow-through, wash, and all elutions were analyzed on 15% SDS-PAGE for an estimation of concentration before desalting.

Augmented cTnI phosphorylation in SHR

Top-down Mass Spectrometry—Purified cTn complexes were desalted with offline reverse phase C18 protein microtrap (Michrom Bioresources Inc.) and eluted with 1% acetic acid in 30:70, 50:50, and 75:25 methanol:water elution buffer. The sample was then introduced to a linear trap/Fourier transform ion cyclotron resonance (FTICR) mass spectrometer (Thermo Scientific) by an automated nanoelectrospray ionization source (Triversa NanoMate; Advion BioSciences, Ithaca, NY) as described previously (33, 42). 2–3% electron energy and 55-ms duration time were used for ECD. Approximately 2,000 scans with 2 microscans were averaged for each ECD spectrum to ensure data quality.

All MS and MS/MS data were analyzed and assigned to rat cTnI sequence (Swiss-Prot P23693, TNNI3_RAT) using in-house developed ion assignment software. The signal:noise threshold was set at 3 and fit factor at 40%. The tolerance for mass error was 10 ppm for precursor ions and 20 ppm for fragment ions, respectively. All reported mass values are most abundant masses. Allowances were made for PTMs such as removal of N-terminal methionine, acetylation, and phosphorylation. The mass lists generated for ECD analysis were manually validated and assigned to fragments with or without modifications.

Quantitative analysis was performed as described previously (32, 33, 41, 42). Briefly, the integrated peak heights of the top five isotopomers were used to calculate the relative abundance of each observed protein or fragment ion. The percentages of the mono- ($\%P_{\text{mono}}$), bis- ($\%P_{\text{bis}}$), and tris- ($\%P_{\text{tris}}$) phosphorylated cTnI species are defined as the summed abundances of mono-phosphorylated cTnI (${}_p\text{cTnI}$), bis-phosphorylated cTnI (${}_{pp}\text{cTnI}$), and tris-phosphorylated (${}_{ppp}\text{cTnI}$) species over the summed abundances of the entire cTnI population, respectively. Equation 1 (Eq. 1) is used to calculate the quantitative value of the total amount of cTnI phosphorylation (P_{total} , mol of Pi/mol of cTnI),

$$P_{\text{total}} = (\%P_{\text{mono}} + 2 \times \%P_{\text{bis}} + 3 \times \%P_{\text{tris}})/100 \quad (\text{Eq. 1})$$

Samples were run in triplicate to ensure technical consistency, and averages were taken for statistical analysis. The percentages of phosphorylation were analyzed and plotted using Prism 5.0 (GraphPad Software).

Statistical Analysis—Data are expressed as mean \pm S.E. Student's *t* tests were performed between group comparisons to evaluate statistical significance of variance. Differences among means were considered significant at $p < 0.05$.

RESULTS

Characterization of SHR Heart Failure—SHRs develop high blood pressure early on (~ 8 – 10 weeks) and remain hypertensive throughout their lifespan. At ~ 80 weeks, SHRs (referred to as SHR-HF hereafter) showed significantly higher systolic blood pressure compared with normotensive WKY (Fig. 1A). SHR-HFs also demonstrated a progressive increase in heart weight and a decrease in body weight compared with age-matched WKY. The ratio of heart weight to body weight is significantly higher in SHRs than that of age-matched WKY, indicating severe hypertrophy (Fig. 1B).

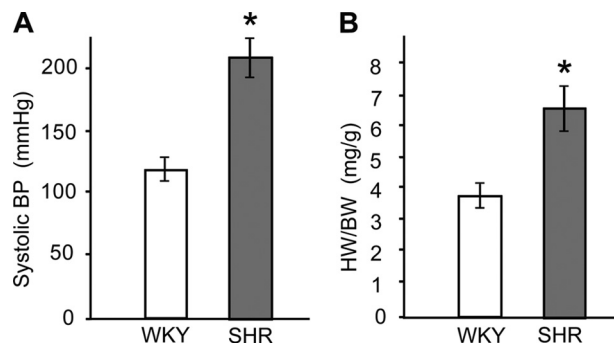


FIGURE 1. **Characteristics of SHR-HF versus WKY.** A, systolic blood pressure in SHR versus WKY at 80 weeks. B, ratio of heart weight (HW) to body weight (BW) of SHR versus WKY.

SDS-PAGE and High Resolution MS Analysis of cTnI from WKY and SHR—We employed immunoaffinity chromatography for the purification of cTn complex from both WKY and SHR-HF left ventricular tissue samples. Representative SDS-PAGE of the affinity purification process is shown in [supplemental Fig. S1](#). As the three subunits of cTn strongly interact with each other, cTnT and cTnC co-elute with cTnI that binds tightly to the anti-cTnI antibody. The three bands at ~ 37 , 26, and 18 kDa correspond to cTnT, cTnI, and cTnC, respectively.

In parallel to SDS-PAGE analysis, the affinity-purified cTn heterotrimer was separated with off-line reverse-phase protein chromatography and analyzed by top-down MS. MS spectra of cTnI from the WKY and SHR-HF groups exhibit large difference in the phosphorylation level (Fig. 2). In WKY, cTnI is present in three forms: un-, mono- and bis-phosphorylated, with mass increment of 80 Da (the mass of added phosphate, HPO_3) between each other. The most abundant molecular mass of 24,069.97 Da matches well with the unphosphorylated cTnI based on the rat cTnI sequence (Swiss-Prot P23693, TNNI3_RAT) with the removal of initial methionine and N-terminal acetylation (calculated: 24,069.73 Da). The other two masses, 24,149.93 and 24,229.87 Da, are consistent with mono- and bis-phosphorylated cTnI (calculated: 24,149.69 and 24,229.66 Da), respectively. Evidently, the majority of cTnI exists as unphosphorylated in WKY. Tris-phosphorylated cTnI is not detected in WKY myocardium (which is estimated to be $< 0.1\%$ of the total cTnI population based on the signal intensity at the expected position of tris-phosphorylated cTnI over the summed intensity of all cTnI protein forms). In contrast, SHR-HF exhibits significant hyperphosphorylation of cTnI. The relative intensity of bis-phosphorylated cTnI is significantly increased in SHR-HF compared with WKY. Tris-phosphorylated cTnI, which has an experimental molecular mass of 24,309.85 Da and is 80 Da larger than the bis-phosphorylated protein, was confidently detected in SHR-HF. The single amino acid polymorphism of S7A reported in our previous study in cTnI purified from Sprague-Dawley rats (48) was not detected in WKY or SHR hearts.

Top-down Quantitative MS Analysis—To satisfy statistical requirements, we have systematically analyzed cTnI purified from 7 WKY and 7 SHR-HF hearts. Three technical replicates were performed for each sample to ensure data reproducibility and consistency. cTnI from all SHR-HF hearts shows consis-

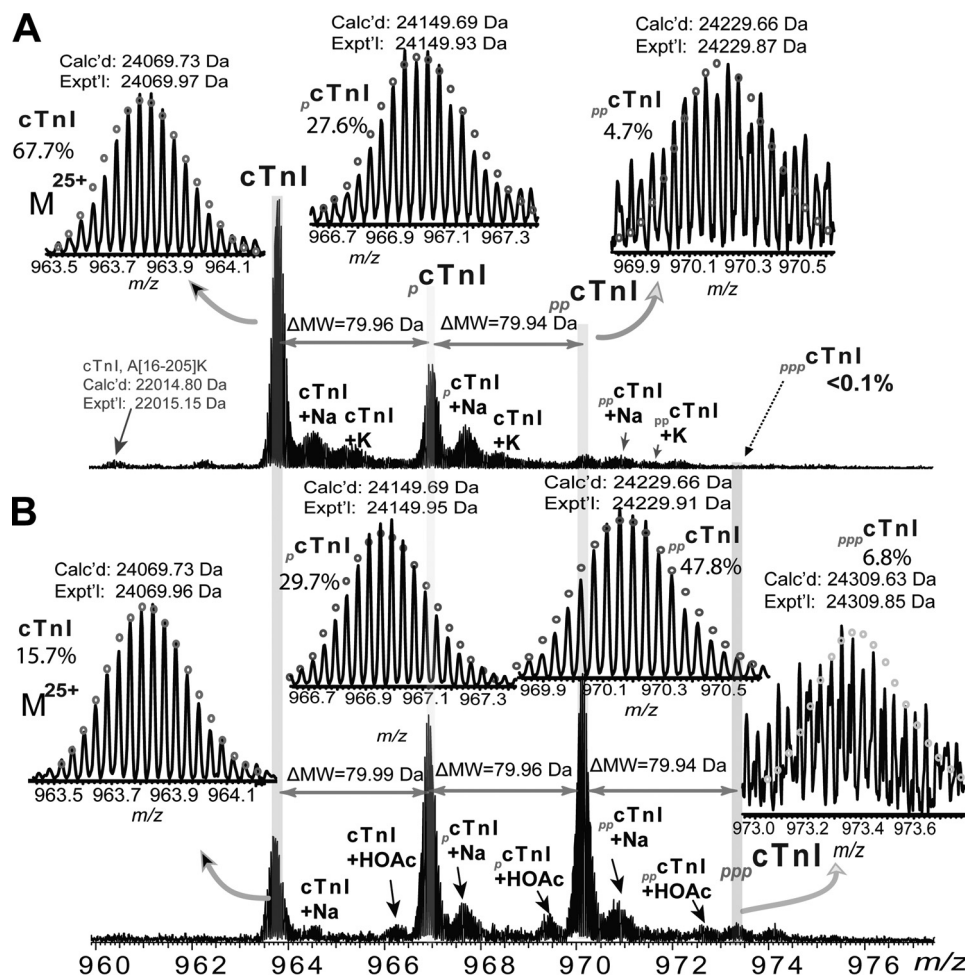


FIGURE 2. High resolution FTMS analysis of intact rat cTnI purified from WKY and SHR. *A*, representative FTMS spectrum of cTnI (M^{25+}) purified from age-matched WKY. Dashed arrow indicates the expected position of tris-phosphorylated cTnI (ppp cTnI) which is not observed in this spectrum. The minor proteolytic fragment, cTnI A(16–205)K, was observed. *B*, FTMS spectrum of cTnI purified from SHR-HF. ppp cTnI was observed in this spectrum. Circles represent theoretical isotopic abundance distribution of the isotopomer peaks. p cTnI, mono-phosphorylated cTnI; pp cTnI, bis-phosphorylated cTnI. ΔMW , molecular mass difference. +Na, sodium adduct; +K, potassium adduct; +H₃PO₄, noncovalent phosphoric acid adduct; +HOAc, noncovalent acetic acid adduct. *Calc'd*, calculated most abundant mass; *Expt'l*, experimental most abundant mass.

tently higher bis-phosphorylation than WKY. Percentages of mono- and bis-phosphorylation from WKY and SHR are shown in Fig. 3, *A* and *B*, respectively. The percentages of mono-phosphorylated cTnI ($\%P_{\text{mono}}$) are comparable between WKY and SHR (WKY $34.3\% \pm 7.6\%$, SHR $37.5\% \pm 4.9\%$, Student's *t* test $p = 0.1825$), whereas the percentages of the bis-phosphorylated form ($\%P_{\text{bis}}$) differ drastically between the two groups (WKY $7.2\% \pm 6.3\%$, SHR $31.5\% \pm 8.3\%$, Student's *t* test $p < 0.001$). The tris-phosphorylated form is only present in SHR ($\%P_{\text{tri}}$, $3.7\% \pm 2.4\%$). The total amount of cTnI phosphorylation (P_{total} , mol Pi/mol cTnI) is shown in Fig. 3C. The difference between WKY and SHR is of high statistical significance (WKY 0.49 ± 0.06 , SHR 1.12 ± 0.07 , Student's *t* test $p < 0.001$), which shows that SHR cTnIs are hyperphosphorylated compared with WKY.

Localization of cTnI Phosphorylation Sites by ECD—To identify the augmented phosphorylation sites and assess the order of phosphorylation, single charge states of mono-phosphorylated cTnI of WKY, mono- and bis-phosphorylated cTnI of SHR-HF, were individually isolated in the mass spectrometer by gas-phase purification (supplemental Fig. S2). The precursor

ions were then dissociated by ECD and generated a series of fragmented product ions. The summary of three ECD datasets for mono-phosphorylated WKY cTnI, mono-phosphorylated SHR-HF cTnI, and bis-phosphorylated SHR-HF cTnI indicates full sequence coverage (Fig. 4). Overall, the total numbers of ions generated for mono-phosphorylated WKY cTnI were 31 *c* ions and 63 *z'* ions (Fig. 4A); 64 *c* ions and 85 *z'* ions for mono-phosphorylated SHR-HF cTnI (Fig. 4B); and 49 *c* ions and 78 *z'* ions for bis-phosphorylated SHR cTnI (Fig. 4C). Note that *c* ions counts from the N terminus and *z'* counts from the C terminus (e.g. c_{21} covers the first 21 amino acids from the N terminus (residues 1–21), and z'_{21} covers the first 21 amino acids from the C terminus (residues 190–210)).

Supplemental Fig. S3 displays some key ions used for mapping the phosphorylation sites. The top panels (supplemental Fig. S3, A1–H1) show fragment ions from mono-phosphorylated cTnI of WKY, and the lower two panels (supplemental Fig. S3, A2–H2 and A3–H3) show fragments from mono- and bis-phosphorylated cTnI of SHR-HF, respectively. In mono-phosphorylated WKY spectra, no ions before c_{21} are phosphorylated (Fig. 4A and supplemental Fig. S3, A1). c_{22} remains un-phos-

Augmented cTnI phosphorylation in SHR

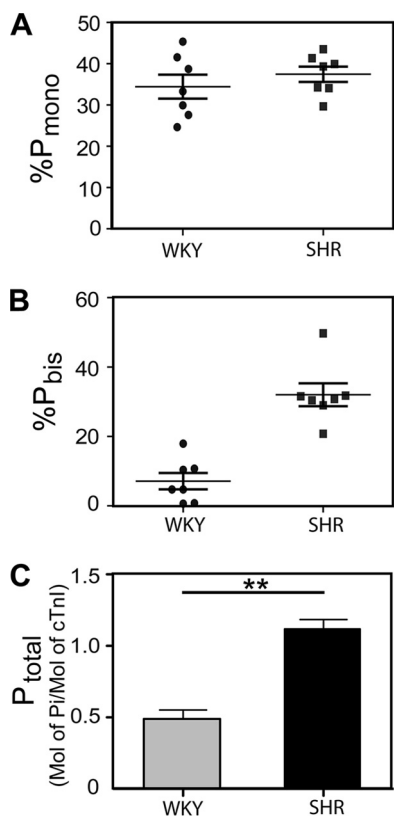


FIGURE 3. Quantification of cTnI phosphorylation in WKY and SHR-HF hearts. The percentages of mono-phosphorylated cTnI components (%P_{mono}) are shown in *A*, and the percentages of bis-phosphorylated cTnI (%P_{bis}) are shown in *B*. Each data point indicates average of triplicates. The total amount of cTnI phosphorylation (P_{total}, mol Pi/mol cTnI) is shown in *C*. Data are expressed as mean ± S.E. *, *p* < 0.05; **, *p* < 0.001.

phosphorylated (supplemental Fig. S3, B1) whereas all ions after *c*₂₃ are detected in their mono-phosphorylated forms (supplemental Fig. S3, C1–H1). These results suggest that Ser²³ is the primary phosphorylation site in WKY mono-phosphorylated cTnI.

We analyzed the ECD spectra of SHR-HF mono- and bis-phosphorylated cTnI (Fig. 4, B and C). Similar to that of WKY, *c* ions before *c*₂₁ are exclusively unphosphorylated in SHR mono-phosphorylated cTnI (Fig. 4B and supplemental Fig. S3, A2). The *c*₂₂ ion was also detected in its unphosphorylated form (supplemental Fig. S3, B2), but only mono-phosphorylated *c* ions were observed after *c*₂₃ (supplemental Fig. S3, C2–H2), which suggests that Ser²³ is the primary phosphorylation site in mono-phosphorylated SHR-HF cTnI. In the ECD of SHR bis-phosphorylated cTnI spectra, *c*₂₂ is majorly mono-phosphorylated, with approximately 35% in the unphosphorylated form. This suggests that there are other potential phosphorylation sites beyond Ser^{22/23}. Consistently, ions between *c*₂₃ and *c*₄₁ in these spectra exhibit approximately 26–36% (31 ± 4%) mono-phosphorylated signal (Fig. 4C and supplemental Fig. S3, C3–E3). On the other hand, all fragments larger than *c*₄₁ (*i.e.* *c*₄₆, *c*₄₈, and *c*₆₇) (supplemental Fig. S3, F3–H3) show bis-phosphorylated forms exclusively, and mono-phosphorylated peaks were not positively detected. As shown in supplemental Fig. S2, the isolation spectra were clean so these signals should come from the bis-phosphorylated protein. Collectively, these results

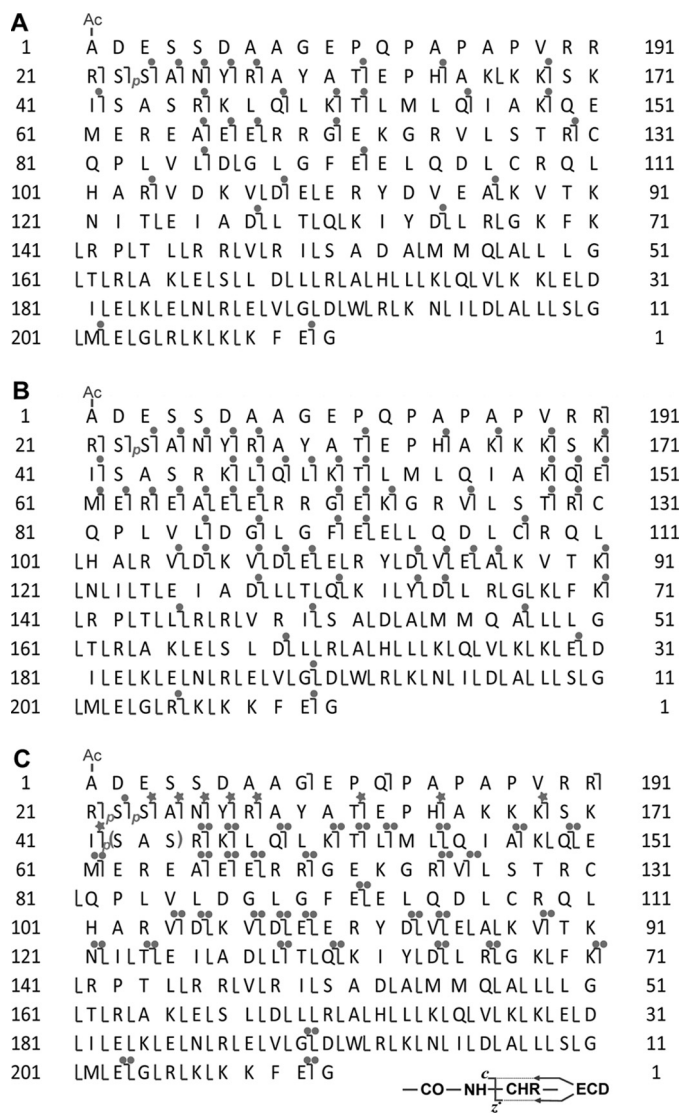


FIGURE 4. Identification of cTnI phosphorylation sites in WKY and SHR-HF. A–C, ECD product maps from WKY mono-phosphorylated cTnI (*A*), SHR-HF mono-phosphorylated cTnI (*B*), and bis-phosphorylated SHR-HF cTnI (*C*). Fragment assignments were made to DNA-predicted rat cTnI sequence (Swiss-Prot P23693, TNNI3_rat) with the removal of N-terminal methionine and acetylation at the new N terminus. *Single dot*, only mono-phosphorylated ions observed. *Double dots*, only bis-phosphorylated ions observed. *Star*, both mono- and bis-phosphorylated ions observed. Identified phosphorylation sites are labeled as *p*.

indicate that there are phosphorylation sites between the 41st and 46th amino acids. In this region, Ser⁴² and Ser⁴⁴ are the only possible sites for phosphorylation and are also well known targets of PKC.

In summary, top-down ECD MS identified Ser²³ as the phosphorylation site in mono-phosphorylated cTnI. Ser^{22/23} is also identified as the major phosphorylation sites in the bis-phosphorylated cTnI. However, phosphorylation is not exclusive to these two cTnI sites. Ser^{42/44} has been detected as the minor phosphorylation sites in SHR-HF. The fact that Ser^{42/44} was only phosphorylated in bis-phosphorylated cTnI but not in mono-phosphorylated cTnI suggests a possible interdependence between Ser^{22/23} and Ser^{42/44}.

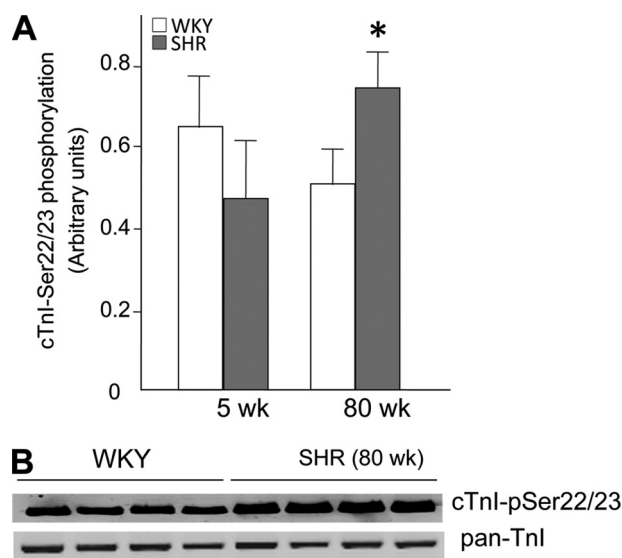


FIGURE 5. Differential phosphorylation of cTnI-Ser^{22/23} in SHR-HF and WKY. *A*, analysis of site-specific phosphorylation of cTnI-Ser^{22/23} in cardiac myofibrils isolated from 5-week-old (*wk*) and 80-week-old hearts. Data are means \pm S.E. (error bars) of the values calculated from the optical density of the bands obtained by immunoblotting normalized against pan-cTnI densities ($n = 8$ hearts/group). Values marked with an asterisk were deemed statistically significant ($p < 0.05$). *B*, Representative immunoblots show reactivity of antiphosphorylation-specific antibodies cTnI-Ser^{22/23} with freshly isolated cardiac myofibrils from 80-week-old animals ($n = 8$ hearts). Each lane represents a distinct heart.

Analysis of Site-specific cTnI Phosphorylation by Immunoblotting—We employed immunoblotting to confirm the changes in specific phosphorylation sites in cTnI from SHR and WKY. Analysis of site-specific phosphorylation of cTnI-Ser^{22/23} in cardiac myofibrils isolated from SHR-HF hearts showed a significantly higher level of phosphorylation compared with age-matched WKY (whereas no significant changes were observed in the normotensive 5-week-old SHR and WKY hearts) (Fig. 5*A*). Representative immunoblots show reactivity of anti-cTnI-Ser^{22/23} phosphorylation-specific antibodies with freshly isolated cardiac myofibrils from SHR-HF animals (Fig. 5*B*). These data confirmed our MS result that Ser^{22/23} phosphorylation of cTnI is increased in failing SHR hearts. At an intermediate age (12–13 weeks old) where the animals experience sustained hypertension, Boknik *et al.* observe augmented cTnI phosphorylation at the N-terminal Ser^{22/23} (50). The attempt to confirm Ser^{42/44} phosphorylation in SHR-HF hearts was hampered by poor specificity and reactivity of the anti-cTnI-Ser^{42/44} phosphorylation specific antibodies (Abcam).

Characterization of PKA and PKC Expression Levels in SHR versus WKY—Because cTnI-Ser^{22/23} is the prototypical PKA substrate, we investigated whether PKA expression levels had changed in SHR and WKY hearts. Both PKA types I and II show no significant changes in SHR-HF hearts compared with age-matched WKY (Fig. 6). Our data suggest that the augmented phosphorylation at Ser^{22/23} of cTnI is not directly related to PKA levels.

Ser^{22/23} can also be phosphorylated by PKC- $\alpha/\beta/\epsilon/\delta$ (14, 16, 19, 24), and Ser^{42/44} is known to be the substrate for PKC- α/ϵ (8, 16, 22). Therefore, we used immunoblotting to investigate the expression levels of PKC- $\alpha/\beta/\epsilon/\delta$ in SHR-HF and WKY.

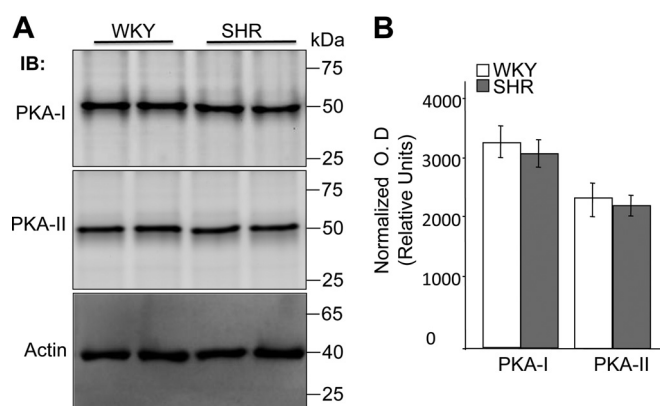


FIGURE 6. PKA type I and II protein levels show no significant change in SHR-HF hearts compared with age-matched WKY. *A*, representative immunoblots from two distinct WKY and SHR-HF hearts are shown. *B*, bar graph data are means of the values calculated from the optical density of the bands obtained by immunoblotting normalized against anti-actin densities ($n = 6$ hearts/group). No statistical significant difference was observed ($p > 0.05$).

Anti-PKC isoform-specific antibodies showed amplified levels of PKC- α and PKC- δ , reduced expression level of PKC- ϵ , but no change in PKC- β in the SHR-HF hearts compared with age-matched WKY (Fig. 7). It is plausible that the augmented phosphorylation of cTnI may be related to the up-regulation of PKC- α/δ .

DISCUSSION

Hyperphosphorylation of cTnI in SHR—We have demonstrated significant increases in cTnI phosphorylation levels in the failing SHR myocardium (80 weeks old) compared with WKY. cTnI from SHR-HF hearts is present in highly abundant mono- and bis-phosphorylated forms and the detection of tris-phosphorylation in SHR-HF indicates the presence of at least three phosphorylation sites in SHR-HF (Fig. 2). Top-down ECD MS unambiguously mapped the cTnI hyperphosphorylation sites to Ser^{22/23} and Ser^{42/44}.

Ser^{22/23} are located on the N-terminal extension that is unique to the cardiac form of TnI and have been shown to be the only sites basally phosphorylated in healthy animals and human myocardium (33, 41, 42, 48). cTnI-Ser^{22/23} phosphorylation dampens myofilament responsiveness to activating Ca²⁺, enhances the rate of relaxation, augments cross-bridge cycling, and accelerates unloaded shortening velocity (51–53). Immunoblot analysis showed no significant changes in PKA levels between SHR and WKY. Therefore, we hypothesized that augmented phosphorylation of cTnI-Ser^{22/23} could be due to up-regulation of the PKC family of kinases. cTnI-Ser^{22/23} phosphorylation is ascribed to various PKC isoforms (α , β , δ) or PKC-activated enzymes (8). Our immunoblot data with anti-PKC isoform-specific antibodies revealed that protein expression of PKC- α/δ is up-regulated whereas PKC- β remains unchanged, and PKC- ϵ is down-regulated in SHR-HF compared with age-matched WKY. These results suggest that augmented phosphorylation of cTnI-Ser^{22/23} is most likely due to up-regulation of PKC- α/δ at the myofilaments.

Ser^{42/44}, traditionally viewed as PKC-specific phosphorylation sites, are the common phosphorylation sites for all PKC isozymes and are known to be preferably regulated by PKC- α

Augmented cTnI phosphorylation in SHR

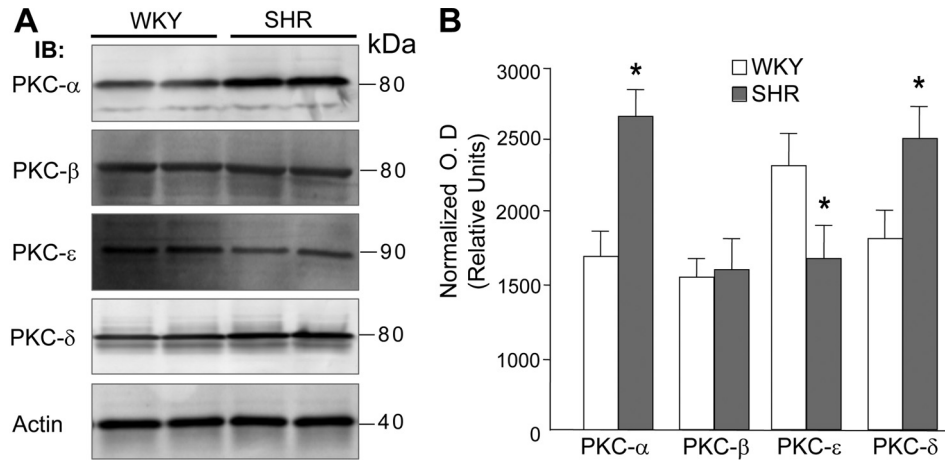


FIGURE 7. **Differential PKC protein levels in the SHR-HF hearts compared with age-matched WKY.** Anti-PKC isoform-specific antibodies show augmentation of PKC- α and PKC- δ , decrease in PKC- ϵ , and no change in PKC- β protein expression levels in SHR-HF hearts. *A*, representative immunoblots (*IB*) from two distinct WKY and SHR-HF hearts. *B*, bar graph data are means of the values calculated from the optical density of the bands obtained by immunoblotting normalized against anti-actin densities ($n = 6$ hearts/group). *, $p < 0.05$.

(16, 22). Ser^{42/44} are located in the “anchor” region near the N terminus of cTnI that interacts directly with the C-terminal lobe of cTnC (4, 9). The functional effects of Ser^{42/44} have been extensively studied by both *in vitro* assays in reconstituted detergent-skinned fiber bundles in which the endogenous cTnI was replaced with specific cTnI mutants and *in vivo* in transgenic animal models in which Ser^{42/44} were rendered unphosphorylatable by mutation to alanine (cTnI-S42A/S44A) or constitutively phosphorylated (*i.e.* pseudo-phosphorylated) by mutation to glutamic acid (cTnI-S42E/S45E/T144E) (8, 15, 16, 54–58). *In vitro* reconstituted skinned fiber preparations show Ser^{42/44} phosphorylation decreases maximal actomyosin Mg-ATPase, Ca²⁺-activated force, cross-bridge cycling rate, and Ca²⁺ sensitivity of force development (8, 15, 16). These effects may increase the cost of contraction and contribute to the loss of mechanical function and eventually could lead to heart failure (11, 16, 54). Roman *et al.* showed that preventing Ser^{42/44} phosphorylation had beneficial, positive inotropic and lusitropic effects on the heart (59). Scruggs *et al.* generated a transgenic mouse line by crossing a PKC- ϵ -overexpressing mouse with the cTnI-S43A/S45A and demonstrated that hyperphosphorylation of the Ser^{42/44} on cTnI is an important contributor to left ventricular dysfunction (56). In addition, Kirk *et al.* suggests that a modest increase (approximate to 7%) in cTnI pseudo-phosphorylation at Ser^{42/44} (together with Thr¹⁴⁴) significantly reduced cardiac muscle contractile function (60). Collectively, these studies indicate that phosphorylation of cTnI by PKC has a detrimental effect on myocardial contractile ability whereas inhibition of PKC-dependent phosphorylation at Ser^{42/44} is beneficial and improves cardiac contractility (59).

Whereas PKA-dependent phosphorylation of Ser^{22/23} sites is taken as fact, PKC-dependent phosphorylation of Ser^{42/44}, until now, was somewhat controversial, mainly due to the lack of *in vivo* evidence (27, 61). Our previous studies using healthy animal and human heart tissues only detected Ser^{22/23} phosphorylation in cTnI (33, 41, 42, 48). Moreover, the cTnI phosphorylation level is significantly lower, and Ca²⁺ sensitivity is higher in skinned myocytes isolated from explanted human hearts

compared with controls (10, 61, 62). Consistently, our recent report employing top-down MS also revealed nearly abolished phosphorylation level of cTnI in failing human hearts compared with healthy controls (49). These findings raised the question of whether the other phosphorylation sites such as Ser^{42/44} are ever phosphorylated *in vivo* and are of any significance pertaining to pathologies in human hearts (27). Remarkably, in the present study we provide the direct evidence that Ser^{42/44} phosphorylation is indeed present *in vivo*, in the myocardium of rats with hypertensive heart failure, suggesting a potentially important role of PKC-mediated phosphorylation in the control of the integrated function of cardiac sarcomeres in certain pathological conditions.

We reason that the discrepancy between the human donor/failing hearts and WKY/SHR-HF hearts can be attributable to species differences (human *versus* rat) and, more importantly, different disease etiologies. The human heart failure samples are from end-stage ischemic/dilated cardiomyopathy or coronary artery diseases (10, 49, 61, 62) whereas SHR-HF samples studied here are purely from hypertension-induced heart failure. Although direct analysis of human heart samples are ideal because the measurements are closest to human cardiac disorders, admittedly, it is challenging to study the disease mechanisms from human samples due to the lack of adequate and proper controls and complication with multiple confounders (heterogeneous disease etiologies associated with co-morbidities and extensive pharmacological treatment especially for the end-stage heart failure patient) (27, 63). In contrast, the animal models offer great advantages, including the ability to precisely control and define disease etiology and stages as well as greatly reduced complexity and heterogeneity. The similarities in chronic stress responses in the animal and human systems suggest that much can be learned from the well controlled animal disease models with the proper consideration of the distinctions between animal and human hearts (64). Conceivably, the findings from animal models can be relevant and shed light on the complex underlying molecular mechanisms of human diseases (27).

We did not observe phosphorylation on Ser⁷⁶/Thr⁷⁷ in WKY/SHR samples. Ser^{76/77} is another potential phosphorylation site previously identified in commercially available human cTnI samples (32). This is consistent with our recent report on human clinical samples (49). Because the commercially available cTnI sample was purified from a mixture of multiple hearts possibly without proper control or preservation, pathologic implication of Ser⁷⁶/Thr⁷⁷ remains to be investigated further.

Altered PKC Expression and Activity in Heart Failure—Augmented PKC-dependent phosphorylation of Ser^{42/44} sites of cTnI in SHR-HF suggests that a dysregulation of the PKC signaling pathway may have an important role in failing myocardium. The PKC family contains at least 12 Ser/Thr kinases (3). PKC isoforms α , β , δ , and ϵ are the best studied among many PKC isozymes expressed in cardiomyocytes. PKC- α is highly expressed in the adult heart, and its expression is elevated in the failing human heart (26) and in end-stage heart failure rat myocytes (25). Cardiac expression and activation of PKC- δ are detrimental to the normal cardiac function (3, 66). No changes were detected for the PKC- β expression level in the animal models of chronic heart failure (25), which is in agreement with our immunoblot data on PKC- β . Regarding PKC- ϵ , many studies showed that the activation of PKC- ϵ is cardioprotective, especially in the context of ischemic preconditioning (3). Inhibition or depletion of PKC- ϵ results in loss of cardioprotection, impaired cardiac function, and the onset of heart failure (67).

Our immunoblot data suggest that PKC- α and δ are up-regulated (whereas PKC- ϵ is down-regulated, and PKC- β protein expression is unchanged in SHR-HF), which contributes, at least in part, to the augmented phosphorylation in Ser^{22/23} and Ser^{42/44}. Increased activity of PKC- α and PKC- δ together with compromised protection by PKC- ϵ appear to be associated with the disease phenotype. PKC activity is induced not only by the α_1 -adrenergic pathway, but also other G_q signaling pathways, most notably AngII (68). The level of AngII is increased in SHR (69–71). Previous studies suggested that PKC regulation is altered in the end-stage human heart failure (3). Inhibition of PKC phosphorylation of cTnI improves cardiac performance *in vivo* (59). Thus, PKC is believed to be a promising therapeutic target for heart failure (3).

A valuable aspect of the SHR studies is the indication that, just like in humans, blockade of angiotensin-converting enzyme or AngII production prevents heart failure development (72). PKC inhibitors were also shown to blunt AngII-induced effects in SHR (73). Evidence from animal and human studies strongly support the idea that PKC activation plays a key role in the hypertensive/failure process both by activating signaling pathways that alter gene expression and by directly phosphorylating myofilament proteins that control cardiac function (3, 74). McCarty collectively referred to the involvement of PKC in SHR as the “PKC syndrome” (36). In SHR, the transition from compensated hypertrophy to failure is accompanied by marked changes in cardiac function, which are associated with altered active and passive mechanical properties of myocardial tissue resulting in a decreased force of contraction. Studies with isolated papillary muscle preparations from SHR *versus* WKY (18–24 month) showed that peak active tension is depressed in SHR groups relative to WKY, whereas the peak intracellular

calcium concentration did not differ between the two groups (65). However, the mechanisms responsible for this depression in function are poorly understood. We propose here a potential mechanism that involves PKC-dependent phosphorylation of cTnI. PKC-dependent cTnI phosphorylation is believed to be particularly important in the development of other hypertrophy/failure syndromes because it is linked to depressed contractile function (5, 27, 55, 56). In agreement with this scenario, our data indicate up-regulation of key PKC isoforms (α and δ) and no change in PKA levels in SHR hearts compared with WKY controls.

PKC activity is kept in balance by protein phosphatases. Whereas the important role of protein phosphatases should be taken into account, the cross-talk between kinases and phosphatases and their sarcomeric targets is poorly understood. Boknik *et al.* (50) indicate that protein phosphatase-1 and -2A expression levels do not change in SHR *versus* WKY myocardium, whereas cTnI phosphorylation is in fact elevated in SHR hearts. This is in agreement with our data.

Top-down ECD MS for Comprehensive Analysis of Protein Phosphorylation—Comprehensive analysis of protein phosphorylation *in vivo* is challenging due to its complex and dynamic nature (63). Top-down MS with ECD is becoming a powerful method for studying phosphorylation *in vivo* (32–34, 42). It measures whole proteins, providing a “bird’s eye” view of all existing modifications in a protein, which can easily and reliably detect the protein phosphorylation by the mass increment of 80 Da (HPO₃). It also offers a relative quantification of protein phosphorylation because the physico-chemical properties of large proteins are much less affected by the presence of phosphorylation group compared with peptides (30–35). Moreover, ECD generates fragment ion-rich data that can be used for quantitative analysis of phosphorylated positional isomers (32). We have demonstrated the unique advantages of top-down ECD MS for comprehensive analysis of protein phosphorylation, including the global detection and quantification of all phosphorylation species simultaneously in one spectrum, and the precise mapping of multiple phosphorylation sites (32–34, 41, 42). Here, we have unambiguously detected and localized all phosphorylation sites in an unbiased manner in WKY and SHR-HF cTnI by the top-down ECD MS approach. The identification of Ser^{42/44} is especially valuable considering the lack of specificity and reactivity of the anti-cTnI-Ser^{42/44} phosphorylation-specific antibodies. We have also quantitatively determined the changes in the distribution of phosphorylation between multiple targeted sites in cTnI from control and failing rat myocardium, which is of crucial importance for understanding protein phosphorylation in cardiac disease (27, 63).

In summary, our study has revealed augmented cTnI phosphorylation levels in SHR-HF compared with age-matched WKY controls using immunoaffinity chromatography, high resolution top-down MS, and Western blot analysis. We have unambiguously identified *in vivo* PKC-specific Ser^{42/44} phosphorylation in the hyperphosphorylated SHR-HF cTnI in addition to Ser^{22/23}. Collectively, our results suggest that cTnI exists in a hyperphosphorylated state in the rat heart with hypertensive heart failure, which is attributable, in part, to alterations in PKC signaling. This study provides the first direct evidence of

Augmented cTnI phosphorylation in SHR

in vivo phosphorylation of Ser^{42/44} sites in cTnI in a clinically relevant animal model of hypertensive heart disease and heart failure. These results support the notion that alterations in PKC signaling may be maladaptive and associated with cardiac dysfunction in hypertensive heart failure.

Acknowledgments—We thank Sijian Wang and Huseyin Guner for assistance in statistical analysis, Lisa Xu and Chad Dooley for helpful discussions, and Raquel Sancho Solis for critical reading of the manuscript.

REFERENCES

- McMurray, J. J., and Pfeffer, M. A. (2005) *Lancet* **365**, 1877–1889
- Mudd, J. O., and Kass, D. A. (2008) *Nature* **451**, 919–928
- Vlahos, C. J., McDowell, S. A., and Clerk, A. (2003) *Nat. Rev. Drug Discov.* **2**, 99–113
- Takeda, S., Yamashita, A., Maeda, K., and Maéda, Y. (2003) *Nature* **424**, 35–41
- Solaro, R. J., Rosevear, P., and Kobayashi, T. (2008) *Biochem. Biophys. Res. Commun.* **369**, 82–87
- Stull, J. T., Brostrom, C. O., and Krebs, E. G. (1972) *J. Biol. Chem.* **247**, 5272–5274
- Pratje, E., and Heilmeyer, L. M. (1972) *FEBS Lett.* **27**, 89–93
- Layland, J., Solaro, R. J., and Shah, A. M. (2005) *Cardiovasc. Res.* **66**, 12–21
- Sumandea, M. P., Burkart, E. M., Kobayashi, T., De Tombe, P. P., and Solaro, R. J. (2004) *Ann. N.Y. Acad. Sci.* **1015**, 39–52
- Messer, A. E., Jacques, A. M., and Marston, S. B. (2007) *J. Mol. Cell. Cardiol.* **42**, 247–259
- van der Velden, J., Papp, Z., Zaremba, R., Boontje, N. M., de Jong, J. W., Owen, V. J., Burton, P. B., Goldmann, P., Jaquet, K., and Stienen, G. J. (2003) *Cardiovasc. Res.* **57**, 37–47
- van der Velden, J., Narolska, N. A., Lamberts, R. R., Boontje, N. M., Borbély, A., Zaremba, R., Bronzwaer, J. G., Papp, Z., Jaquet, K., Paulus, W. J., and Stienen, G. J. (2006) *Cardiovasc. Res.* **69**, 876–887
- Solaro, R. J., Moir, A. J., and Perry, S. V. (1976) *Nature* **262**, 615–617
- Noland, T. A., Jr., Raynor, R. L., and Kuo, J. F. (1989) *J. Biol. Chem.* **264**, 20778–20785
- Noland, T. A., Jr., Guo, X., Raynor, R. L., Jideama, N. M., Averyhart-Fullard, V., Solaro, R. J., and Kuo, J. F. (1995) *J. Biol. Chem.* **270**, 25445–25454
- Jideama, N. M., Noland, T. A., Jr., Raynor, R. L., Blobe, G. C., Fabbro, D., Kazanietz, M. G., Blumberg, P. M., Hannun, Y. A., and Kuo, J. F. (1996) *J. Biol. Chem.* **271**, 23277–23283
- Pi, Y., Kemnitz, K. R., Zhang, D., Kranias, E. G., and Walker, J. W. (2002) *Circ. Res.* **90**, 649–656
- Pi, Y., Zhang, D., Kemnitz, K. R., Wang, H., and Walker, J. W. (2003) *J. Physiol.* **552**, 845–857
- Kobayashi, T., Yang, X., Walker, L. A., Van Breemen, R. B., and Solaro, R. J. (2005) *J. Mol. Cell. Cardiol.* **38**, 213–218
- Robertson, S. P., Johnson, J. D., Holroyde, M. J., Kranias, E. G., Potter, J. D., and Solaro, R. J. (1982) *J. Biol. Chem.* **257**, 260–263
- Westfall, M. V., and Borton, A. R. (2003) *J. Biol. Chem.* **278**, 33694–33700
- Solaro, R. J. (2008) *J. Biol. Chem.* **283**, 26829–26833
- Sumandea, M. P., Rybin, V. O., Hinken, A. C., Wang, C., Kobayashi, T., Harleton, E., Sievert, G., Balke, C. W., Feinmark, S. J., Solaro, R. J., and Steinberg, S. F. (2008) *J. Biol. Chem.* **283**, 22680–22689
- Wang, H., Grant, J. E., Doede, C. M., Sadayappan, S., Robbins, J., and Walker, J. W. (2006) *J. Mol. Cell. Cardiol.* **41**, 823–833
- Belin, R. J., Sumandea, M. P., Allen, E. J., Schoenfelt, K., Wang, H., Solaro, R. J., and de Tombe, P. P. (2007) *Circ. Res.* **101**, 195–204
- Bowling, N., Walsh, R. A., Song, G., Estridge, T., Sandusky, G. E., Fouts, R. L., Mintze, K., Pickard, T., Roden, R., Bristow, M. R., Sabbah, H. N., Mizrahi, J. L., Gromo, G., King, G. L., and Vlahos, C. J. (1999) *Circulation* **99**, 384–391
- Solaro, R. J., and van der Velden, J. (2010) *J. Mol. Cell. Cardiol.* **48**, 810–816
- Kelleher, N. L., Lin, H. Y., Valaskovic, G. A., Aaserud, D. J., Fridriksson, E. K., and McLafferty, F. W. (1999) *J. Am. Chem. Soc.* **121**, 806–812
- Ge, Y., Lawhorn, B. G., ElNaggar, M., Strauss, E., Park, J. H., Begley, T. P., and McLafferty, F. W. (2002) *J. Am. Chem. Soc.* **124**, 672–678
- Sze, S. K., Ge, Y., Oh, H., and McLafferty, F. W. (2002) *Proc. Natl. Acad. Sci. U.S.A.* **99**, 1774–1779
- Han, X., Jin, M., Breuker, K., and McLafferty, F. W. (2006) *Science* **314**, 109–112
- Zabrouskov, V., Ge, Y., Schwartz, J., and Walker, J. W. (2008) *Mol. Cell. Proteomics* **7**, 1838–1849
- Ayaz-Guner, S., Zhang, J., Li, L., Walker, J. W., and Ge, Y. (2009) *Biochemistry* **48**, 8161–8170
- Ge, Y., Rybakova, I. N., Xu, Q., and Moss, R. L. (2009) *Proc. Natl. Acad. Sci. U.S.A.* **106**, 12658–12663
- Siuti, N., and Kelleher, N. L. (2007) *Nat. Methods* **4**, 817–821
- McCarty, M. F. (1996) *Med. Hypotheses* **46**, 191–221
- Pesavento, J. J., Bullock, C. R., LeDuc, R. D., Mizzen, C. A., and Kelleher, N. L. (2008) *J. Biol. Chem.* **283**, 14927–14937
- Jiang, L., Smith, J. N., Anderson, S. L., Ma, P., Mizzen, C. A., and Kelleher, N. L. (2007) *J. Biol. Chem.* **282**, 27923–27934
- Ryan, C. M., Souda, P., Bassilian, S., Ujwal, R., Zhang, J., Abramson, J., Ping, P., Durazo, A., Bowie, J. U., Hasan, S. S., Baniulis, D., Cramer, W. A., Faull, K. F., and Whitelegge, J. P. (2010) *Mol. Cell. Proteomics* **9**, 791–803
- Zubarev, R. A., Horn, D. M., Fridriksson, E. K., Kelleher, N. L., Kruger, N. A., Lewis, M. A., Carpenter, B. K., and McLafferty, F. W. (2000) *Anal. Chem.* **72**, 563–573
- Xu, F., Xu, Q., Dong, X., Guy, M., Guner, H., Hacker, T. A., and Ge, Y. (2011) *Int. J. Mass Spectrom.* **305**, 95–102
- Zhang, J., Dong, X., Hacker, T. A., and Ge, Y. (2010) *J. Am. Soc. Mass Spectrom.* **21**, 940–948
- Okamoto, K., and Aoki, K. (1963) *Jap. Circ. J.* **27**, 282–293
- Bing, O. H., Conrad, C. H., Boluyt, M. O., Robinson, K. G., and Brooks, W. W. (2002) *Heart Fail. Rev.* **7**, 71–88
- Bing, O. H., Brooks, W. W., Robinson, K. G., Slawsky, M. T., Hayes, J. A., Litwin, S. E., Sen, S., and Conrad, C. H. (1995) *J. Mol. Cell. Cardiol.* **27**, 383–396
- Sfichi-Duke, L., Garcia-Cazarin, M. L., Sumandea, C. A., Sievert, G. A., Balke, C. W., Zhan, D. Y., Morimoto, S., and Sumandea, M. P. (2010) *J. Mol. Cell. Cardiol.* **48**, 934–942
- Sumandea, C. A., Garcia-Cazarin, M. L., Bozio, C. H., Sievert, G. A., Balke, C. W., and Sumandea, M. P. (2011) *J. Biol. Chem.* **286**, 530–541
- Sancho Solis, R., Ge, Y., and Walker, J. W. (2008) *J. Muscle Res. Cell Motil.* **29**, 203–212
- Zhang, J., Guy, M. J., Norman, H. S., Chen, Y. C., Xu, Q., Dong, X., Guner, H., Wang, S., Kohmoto, T., Young, K. H., Moss, R. L., and Ge, Y. (2011) *J. Proteome Res.* **10**, 4054–4065
- Boknik, P., Heinroth-Hoffmann, I., Kirchhefer, U., Knapp, J., Linck, B., Lüss, H., Müller, T., Schmitz, W., Brodde, O., and Neumann, J. (2001) *Cardiovasc. Res.* **51**, 717–728
- Kranias, E. G., and Solaro, R. J. (1982) *Nature* **298**, 182–184
- Kentish, J. C., McCloskey, D. T., Layland, J., Palmer, S., Leiden, J. M., Martin, A. F., and Solaro, R. J. (2001) *Circ. Res.* **88**, 1059–1065
- Strang, K. T., Sweitzer, N. K., Greaser, M. L., and Moss, R. L. (1994) *Circ. Res.* **74**, 542–549
- Montgomery, D. E., Wolska, B. M., Pyle, W. G., Roman, B. B., Dowell, J. C., Buttrick, P. M., Koretsky, A. P., Del Nido, P., and Solaro, R. J. (2002) *Am. J. Physiol. Heart Circ. Physiol.* **282**, H2397–2405
- Pyle, W. G., Sumandea, M. P., Solaro, R. J., and De Tombe, P. P. (2002) *Am. J. Physiol. Heart Circ. Physiol.* **283**, H1215–1224
- Scruggs, S. B., Walker, L. A., Lyu, T., Geenen, D. L., Solaro, R. J., Buttrick, P. M., and Goldspink, P. H. (2006) *J. Mol. Cell. Cardiol.* **40**, 465–473
- Kirk, J. A., MacGowan, G. A., Evans, C., Smith, S. H., Warren, C. M., Mamidi, R., Chandra, M., Stewart, A. F. R., Solaro, R. J., and Shroff, S. G. (2009) *Circ. Res.* **105**, 1232–1239
- Burkart, E. M., Sumandea, M. P., Kobayashi, T., Nili, M., Martin, A. F., Homsher, E., and Solaro, R. J. (2003) *J. Biol. Chem.* **278**, 11265–11272
- Roman, B. B., Goldspink, P. H., Spaite, E., Urboniene, D., McKinney, R.,

- Geenen, D. L., Solaro, R. J., and Buttrick, P. M. (2004) *Am. J. Physiol. Heart Circ. Physiol.* **286**, H2089–2095
60. Kirk, J. A., MacGowan, G. A., Evans, C., Smith, S. H., Warren, C. M., Mamidi, R., Chandra, M., Stewart, A. F., Solaro, R. J., and Shroff, S. G. (2009) *Circ. Res.* **105**, 1232–1239
61. Marston, S. B., and Walker, J. W. (2009) *J. Muscle Res. Cell Motil.* **30**, 93–95
62. Messer, A. E., Gallon, C. E., McKenna, W. J., Dos Remedios, C. G., and Marston, S. B. (2009) *Proteomics Clin. Appl.* **3**, 1371–1382
63. Marston, S. B., and de Tombe, P. P. (2008) *J. Mol. Cell. Cardiol.* **45**, 603–607
64. Walker, J. W. (2006) *J. Mol. Cell. Cardiol.* **40**, 446–450
65. Bing, O. H., Brooks, W. W., Conrad, C. H., Sen, S., Perreault, C. L., and Morgan, J. P. (1991) *Circ. Res.* **68**, 1390–1400
66. Simonis, G., Honold, J., Schwarz, K., Braun, M. U., and Strasser, R. H. (2002) *Basic Res. Cardiol.* **97**, 223–231
67. Gray, M. O., Karliner, J. S., and Mochly-Rosen, D. (1997) *J. Biol. Chem.* **272**, 30945–30951
68. Kang, M., Chung, K. Y., and Walker, J. W. (2007) *Physiology* **22**, 174–184
69. Schunkert, H., Jackson, B., Tang, S. S., Schoen, F. J., Smits, J. F., Apstein, C. S., and Lorell, B. H. (1993) *Circulation* **87**, 1328–1339
70. Studer, R., Reinecke, H., Müller, B., Holtz, J., Just, H., and Drexler, H. (1994) *J. Clin. Invest.* **94**, 301–310
71. Sun, Y., Cleutjens, J. P., Diaz-Arias, A. A., and Weber, K. T. (1994) *Cardiovasc. Res.* **28**, 1423–1432
72. Brooks, W. W., Bing, O. H., Robinson, K. G., Slawsky, M. T., Chaletsky, D. M., and Conrad, C. H. (1997) *Circulation* **96**, 4002–4010
73. Salas, M. A., Vila-Petroff, M. G., Palomeque, J., Aiello, E. A., and Mattiazzi, A. (2001) *J. Mol. Cell. Cardiol.* **33**, 1957–1971
74. Salazar, N. C., Chen, J., and Rockman, H. A. (2007) *Biochim. Biophys. Acta* **1768**, 1006–1018